

Snow microphysical retrieval from dual-wavelength radar measurements

Wanda Szyrmer and Isztar Zawadzki

Department of Atmospheric and Oceanic Sciences, McGill University, Canada H3A 2K6

Corresponding author: Isztar Zawadzki, 805 Sherbrooke St. W, Montreal, QC, H3A 2K6; isztar.zawadzki@mcgill.ca

1-Introduction

To derive quantitative meteorological information from the radar backscattering signal a good knowledge of the microphysical properties of the radar targets is needed. Alas, the exact description of microphysics is elusive due to its complexity. Thus, we always revert to some kind of simplified model of microphysics. The first example is the simplification implied in a Z-R relationship. We are interested here in the use of information provided by X and W-band collocated vertically pointing radars to study snow microphysics. For this we must combine the measurements with model microphysics.

The latter has two main applications: in quantitative interpretation of radar measurements (retrievals), as here, and in numerical modelling. In both instances it is imperative to assess the errors in the model and their impacts on retrievals and on numerical weather prediction (NWP). In Lee et al. (2007) we have made a first attempt at incorporating microphysical model uncertainties into generating “ensemble measurements of precipitation”. These ensembles were based on the statistical properties of the time-space errors in

the Z-R relationship. More recently, we have established a more complete error structure of measurements of precipitation at ground that can be used as the basis for a more realistic generation of ensemble measurements (Berenguer and Zawadzki 2008).

In this paper we further carry these ideas. In our attempt to properly assess the effect of model uncertainty on the retrieval we are led to *ensemble retrievals* of the microphysical properties of observed snow. The ensemble is determined by the spread of uncertainties in the microphysical models derived from past studies.

2-Data

Figure 1 shows the case chosen for this study. The X-band radar is calibrated with distrometer in rain and has shown good stability over periods of some months. At the maximum detectable height of the X-band (close to -15 dBZ) the calibration of the W-band was adjusted assuming that Rayleigh scattering applies to the two (collocated) radars. The trails were straightened by a proper time data-shifting as a function of height.

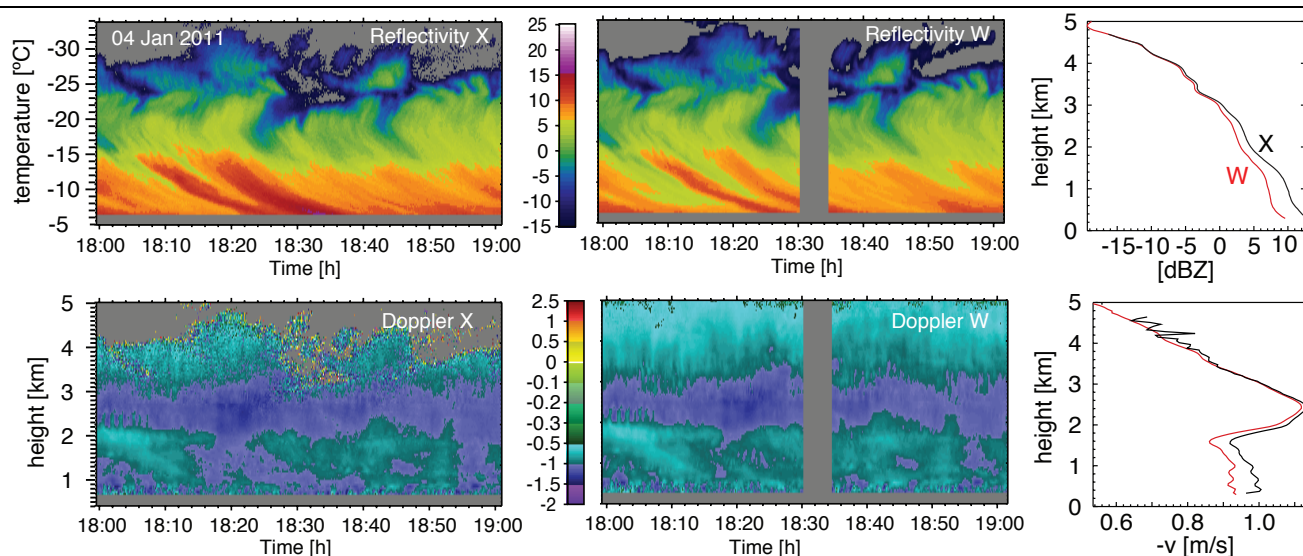


Fig. 1- One hour of the four measured values and their time averages (right). The temperature scale on the reflectivity height–time profile is obtained using the RUC analysis. $Z^{(W)}$ is smoothed in time to match the lower resolution of the X-band radar and it is shown thresholded to the detectable level of $Z^{(X)}$. Forty minutes during the most intense period were analyzed.

3-Model

The four equations that represent the above measurements are:

$$Z_e^{(x)} = 3.2^4 / (0.93\pi^5) \int \sigma_x(D) n(D) dD; \quad Z_e^{(w)} = 0.32^4 / (0.93\pi^5) \int \sigma_w(D, \rho_s(D)) n(D) dD \quad (1)$$

$$U^{(X)} = w - \frac{1}{\int \sigma_x(D) n(D) dD} \int U(D) \sigma_x(D) n(D) dD; \quad U^{(W)} = w - \frac{1}{\int \sigma_w(D, \rho_s) n(D) dD} \int U(D) \sigma_w(D, \rho_s(D)) n(D) dD$$

The unknowns are: $n(D)$, $\rho_s(D)$, $u(D)$ and w , the particle distribution with size D (PSD), particle density, terminal fall velocity and vertical air motion, respectively. The first three are complex functions of size and consequently a simplifying model of snow characteristics is required. We express the PSD in a normalized form: $n(D) = N_0^* h(x)$ where $N_0^* = M_2^4 M_3^{-3}$, $x = DM_2 / M_3 = D / D_{23}$, $h(x)$ is a generic function and M_n is the n^{th} moment of the PSD. We want to retrieve N_0^* and D_{23} . Several generic functions (Fig.2) were derived from results reported in literature: three forms of the Generalized Gamma function with the following parameters: PSD_{GG}: $\mu=-1, \nu=3$; PSD_{G3}: $\mu=3, \nu=1$; PSD_{Exp}: $\mu=0, \nu=1$ (Delanoë et al., 2005) and the parameterization given by Field et al. (2007). In addition the same distributions but truncated at $2.5 D_{23}$ are also used. This is our sample of the uncertainty in the model PSD.

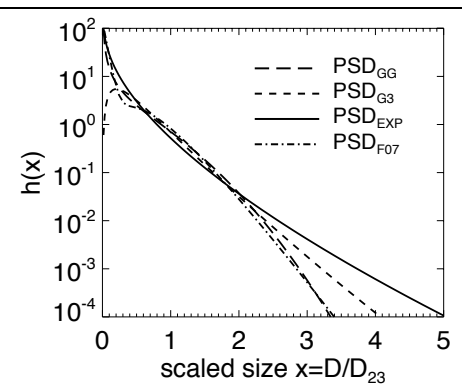


Fig. 2- PSDs used in the retrievals.

It is customary to express the mass-size relationship as a power-law $m(D) = a_m D^{b_m}$, or its equivalent $\rho(D) = a_\rho D^{b_\rho}$. Here again we use a normalized form $m(D) = m^* (D/D^*)^{b_m}$ (or $\rho_s(D) = \rho^* (D/D^*)^{b_m-3}$). We will see that values of

D^* can be determined in such a way as to reduce the sensitivity of results to b_m (we will take $b_m = 2$) and in this way eliminate the uncertainty associated with b_m . We want to retrieve ρ^* . We use four relationships between density and fall speed (Fig. 3): the one obtained by Szyrmer and Zawadzki (2010) and three others derived from information found in literature (Francis et al. 1998; Heymsfield et al. 2004a; Baker and Lawson, 2006; Heymsfield and Westbrook 2010). These various mass-velocity relationships will represent the uncertainty of the model. Thus, fall velocity will be determined from ρ^* and no additional parameters need to be retrieved for fall velocity.

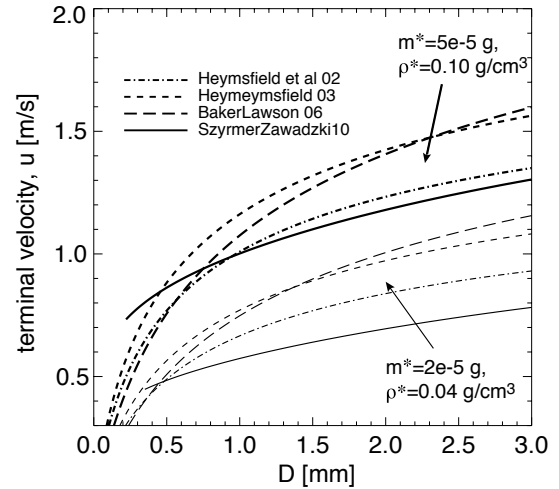


Fig. 3- Four velocity-size relationships obtained from the mass-velocity relationship for two values of ρ^* . The first three have a variable b_m and are used to determine D^* (see below).

The eight PSDs from Fig. 2 and the four velocity-size relationships from Fig. 3 will be the snow model descriptors that define the spread of uncertainty. Each will be used separately for the retrievals. Thus, an ensemble of 32 retrievals will result.

4 Retrieval procedure

Computations of reflectivity were made using model 5 in Fabry and Szyrmer (1999). Uncertain-

ties in computations of W-band reflectivity due to particle shape and orientation were not considered.

The actual retrieval is made sequentially:

First, we determine D^* . Figure 4 shows that by taking $D^* = 1.25$ mm for all the observation pixels with DWR in the interval indicated by the red lines the sensitivity of results to b_m becomes negligible.

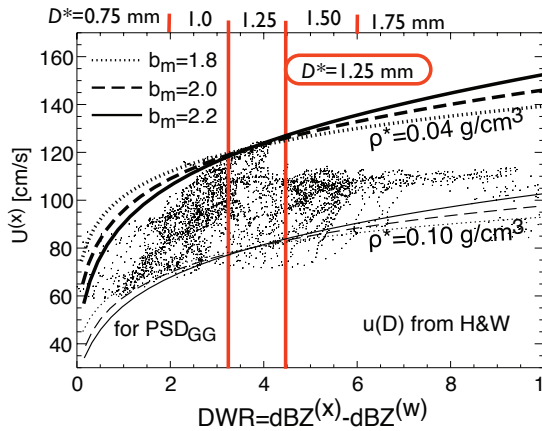


Fig. 4- Dots show all our measurements in the DWR - $U^{(x)}$ space. Curves show computations of these measurements for the indicated of snow model descriptors, in particular for $D^*=1.25$ mm. The variable parameter here is b_m , the exponent in the mass-size relationship. In the interval indicated by the red lines the sensitivity of the computations to b_m is negligible.

For smaller (larger) values of D^* the intersection of the lines moves to the left (right). In this manner we determine, once and for all, five values of D^* (indicated at the top of Fig. 4) sufficient to make retrieval results insensitive to b_m . We then take $b_m = 2$ in the rest of the retrieval. This illustrates the advantage of the normalization of mass-size relationship: it eliminates one of the sources of uncertainty.

We initially assume $w = 0$.

1- D_{23} and ρ^* are determined for every combination of snow model descriptors and those results that match the measured reflectivity difference, DWR, and Doppler velocity of the X-band, $U^{(x)}$ at each pixels are retained. This gives a maximum of 32 ensemble of pairs per pixel.

2- From the X-band reflectivity and the ensemble of the pairs of D_{23} and ρ^* , an ensemble of ice water contents (IWC) is retrieved.

3- An ensemble of N_0^* is derived from IWC, ρ^* and D_{23} . Other derived quantities, such as mean mass-weighted diameter D_m , are also computed.

4- At each pixel all ensemble members with computed values of Doppler velocity difference ($U^{(x)} - U^{(w)}$) $> \pm 3.5$ cm/s of the measured values are rejected.

5- Averages and Standard Deviations (SD) are computed for all retrieved parameters for every pixel in the domain with at least 2 ensemble members retained.

6- Vertical air velocity, w is computed assuming that all water vapor above saturation, generated by w , is immediately deposited on snow and is considered to be equal to the growth of snow measured by the vertical gradient of IWC.

7- With w thus computed the entire retrieval is repeated and a new profile of w is obtained. The retrievals converged after a few iterations.

5 Results

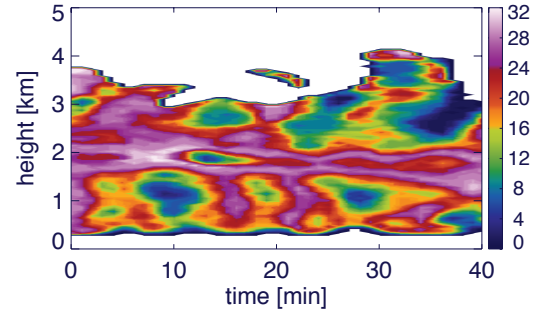


Fig. 5-Number of ensemble members that satisfied all the measurements.

It is interesting that within one hour of observations the number of ensemble members compatible with all radar observations is quite variable in time and space (Fig. 5). In the upper levels none of the included model variations is adequate: either our ensemble spread is too narrow or the measurements at the top are not sufficiently precise (likely both).

In Fig. 6 all the retrieved fields, ensemble average values and their SDs are shown. The averages are well structured which in itself is reassuring since the retrieval is done independently for each pixel. We note that the SDs are also structured indicated that the errors have time-space correlations (one can derive an error correlation matrix in this description of snow).

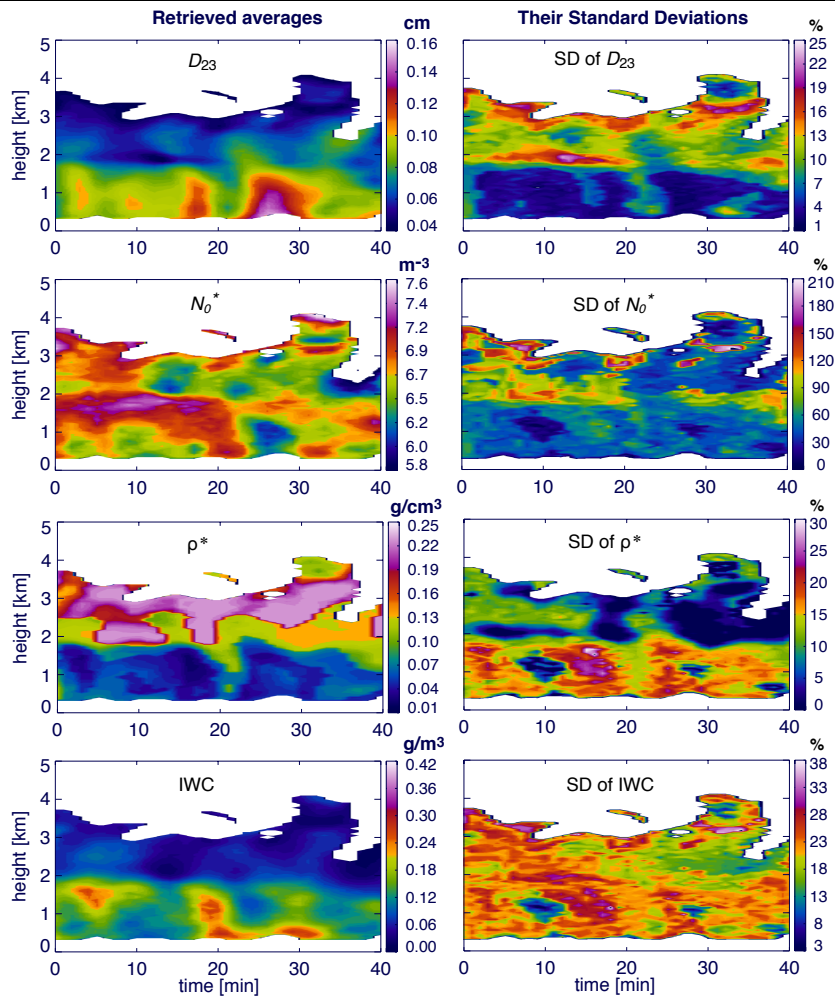


Fig. 6- Top four panels show the fields of ensemble averages of retrieved values of characteristic size, particle density, and IWC and number concentration. The bottom six panels are the fields of their uncertainty.

Note that retrieved snow density increases with fallen height at the same time as the characteristic size increases, which is compatible with aggregation. The IWC sharply increases at ~ 2 km (-15°C) and it is accompanied by an intriguing increase in number concentration indicating that aggregation was not the only active process. Figure 7 shows the vertical air velocity compatible with increase of IWC. Note the sustained maximum at 2 km.

5. Verification

This is the most difficult task in any meteorological work and in particular in remote sensing studies. Here we use the one additional information in the observations not used in the

retrievals, namely Doppler spectra, to explain and verify, to a degree, certain aspects of the retrieved

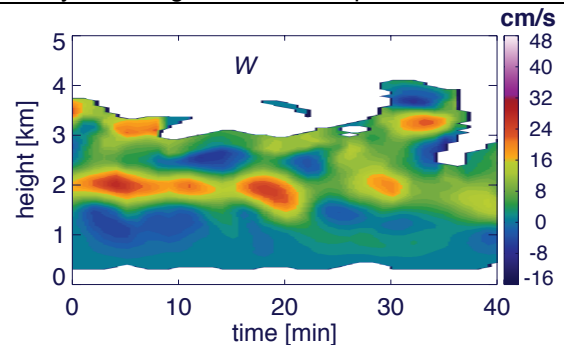


Fig. 7- Updraft compatible with the retrievals in Fig. 6. Maximum values are below 20 cm/s.

results. The sample spectrum in Fig. 8 (representative of the entire period) shows a striking bimodality starting just above 2 km (-15°C level).

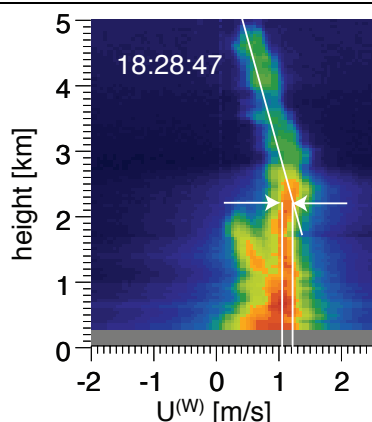


Fig. 8- A sample Doppler spectrum of the W-band radar. Similar spectra were present throughout the entire period of analysis.

At the same time the fall velocity of snow contributing to the original mode decreases by about 15 cm/s (shown by the white lines), consistent with the retrieved updraft. The secondary peak shows the increase in number concentration as result of activation of freezing nuclei not activated previously and resulting from the increase of water vapor. The alternative possibility, generation of supercooled water would require a stronger updraft given the values of the retrieved IWC. This explains the increase in N_0^* . The newly generated particles at around -15°C undergo dendritic growth and consequently a slower fall speed than the more compact particles generated aloft this favors aggregation. The old particles will also be slowed down to the less dense dendritic growth. It all leads to the retrieved decrease of particle density and the broadening of the PSD as seen in the increase of the retrieved characteristic size. Note on the spectrum that slow particles continue to be present all the way to the ground.

The activation of ice nuclei likely occurs in supersaturation. This contradicts the hypothesis under which updraft is calculated. At the level of new ice nuclei activation the updraft is probably stronger than indicated if Fig. 7.

6. Few comments

The emphasis here is on the methodology of ensemble retrievals of snow characteristics; lead to results physically realistic. They indicate a great variability in height and time of snow properties.

No single set of snow descriptors applies to all pixels in this limited sample of 40 min, underlining the question of representativity of in-situ measurements.

Some of the advantages of ensemble retrievals are: from such computation the error covariance matrix of microphysical parameterizations can be derived for data assimilation; the propagation of uncertainty when using retrievals in non-linear processes is possible; it allows the evaluation of microphysical models; and so on.

The SDs computed here estimate the uncertainty of the model microphysics only. Data uncertainties were not taken into account here.

References

- Baker, B. and R.P. Lawson, 2006: Improvements indetermination of ice water content from two-dimensional particle imagery. Part I: Image-to-mass relationships. *J. Appl. Meteor. Climatol.*, **45**, 1282-1290.
- Berenguer, M. and I. Zawadzki, 2008: A study of the error covariance matrix of radar rainfall estimates in stratiform rain, *Weather and Forecasting*, **23**, 1085-1101.
- Delanoë, J., A. Protat, J. Testud, D. Bouniol, A. J. Heymsfield, A. Bansemer, P. R. A. Brown and R.M. Forbes, 2005: Statistical properties of the normalized ice particle size distribution. *J. Geophys. Res.*, **110**, D10201, doi:10.1029/2004JD005405
- Fabry, F., and W. Szyrmer, 1999: Modeling of the melting layer. Part II: Electromagnetics, *J. Atmos. Sci.*, **56**, 3593-3600.
- Field P. R., A. J. Heymsfield, and A. Bansemer, 2007: Snow size distribution parameterization for midlatitude and tropical ice clouds., *J. Atmos. Sci.*, **64**, 4346-4365.
- Heymsfield, A.J., 2003: Properties of Tropical and Midlatitude Ice Cloud Particle Ensembles. Part I: Median Mass Diameters and Terminal Velocities. *J. Atmos. Sci.*, **60**, 2573-2591.
- Heymsfield, A.J., S. Lewis, A. Bansemer, J. Iaquinta, L.M. Miloshevich, M. Kajikawa, C. Twohy, and M. R. Poellot, 2002: A general approach for deriving the properties of cirrus and stratiform ice cloud particles. *J. Atmos. Sci.*, **59**, 3-29.
- Heymsfield, A.J., and C.D. Westbrook, 2010: Advancements in the estimation of ice particle fall speeds using laboratory and field measurements. *J. Atmos. Sci.*, **67**, 2469-2482.
- Lee, G.W A. Seed and I. Zawadzki, 2007: Modeling the variability of drop size distribution in space and time. *J. of Appl. Meteorology*. **46**, 742-756.
- Szyrmer, Wanda, and Isztar Zawadzki, 2010: Snow Studies. Part II: Average Relationship between Mass of Snowflakes and Their Terminal Fall Velocity. *J. Atmos. Sci.*, **67**, 3319-3335. doi: 10.1175/2010JAS3390.1